Volume 54 | Number 84 | 28 October 2018 | Pages 11823–11976

ChemComm

Chemical Communications

rsc.li/chemcomm

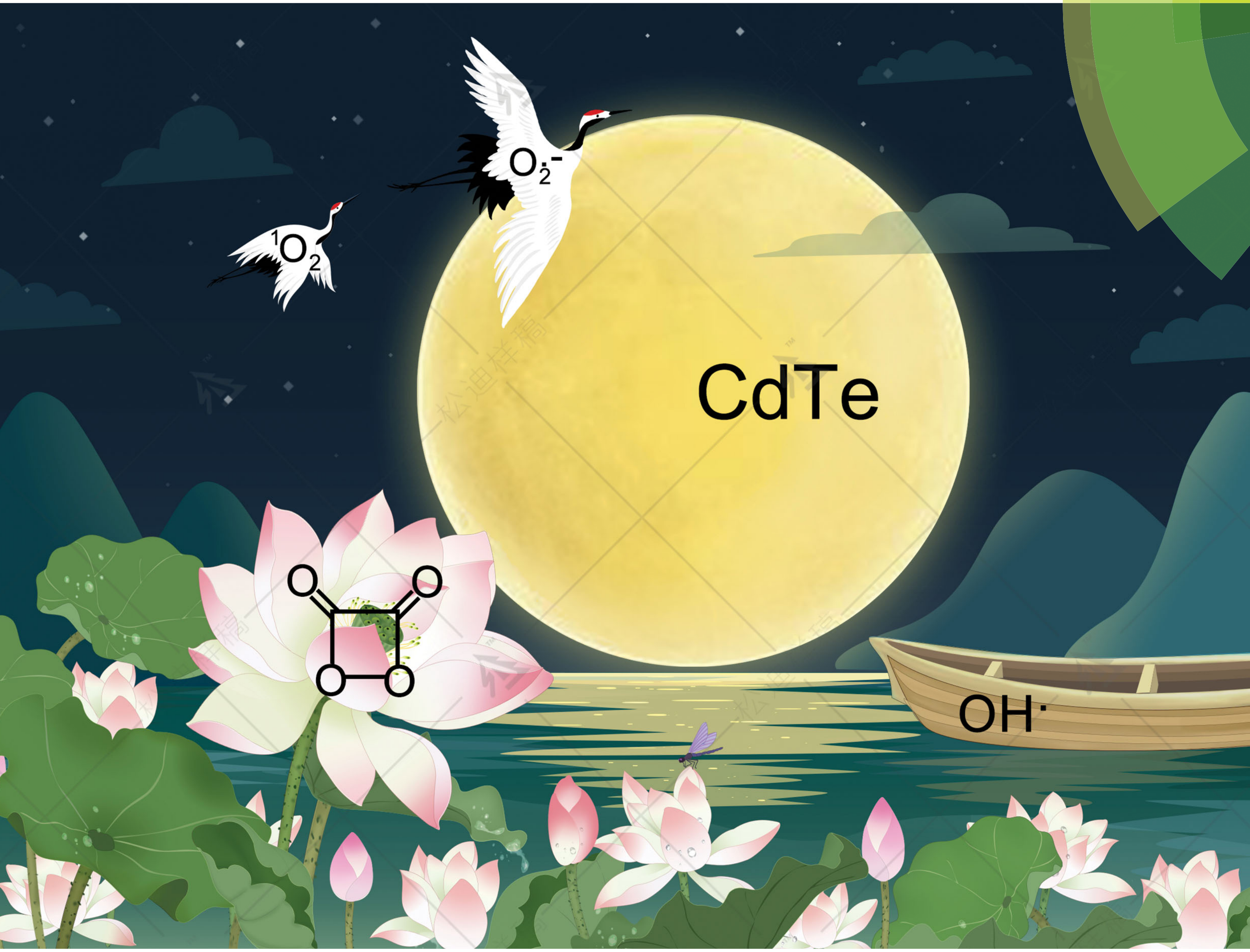

ISSN 1359-7345

ROYAL SOCIETY OF CHEMISTRY

COMMUNICATION
Huangxian Ju *et al.*
Resonance energy transfer and electron–hole annihilation induced chemiluminescence of quantum dots for amplified immunoassay

ChemComm

COMMUNICATION

Cite this: *Chem. Commun.*, 2018, **54**, 11861

Received 3rd August 2018,
Accepted 5th September 2018

DOI: 10.1039/c8cc06356g

rsc.li/chemcomm

Resonance energy transfer and electron–hole annihilation induced chemiluminescence of quantum dots for amplified immunoassay†

Chen Zong,‡[ab] Jie Wu, ‡[a] Yang Zang[a] and Huangxian Ju *[a]

The chemiluminescence (CL) of CdTe quantum dots (QDs) in the presence of peroxyoxalate and hydrogen peroxide was explored and applied for sensitive immunoassay, in which the amplified CL originated from the resonance energy transfer and annihilation of hole-injected and electron-injected QDs.

Chemiluminescence (CL) has served as a powerful analytical tool in the fields of environmental monitoring, clinical diagnosis and drug delivery due to its advantages of simple operation, fast analysis, high sensitivity and a wide linear range.[1,2] Molecular CL systems such as luminol–oxidant–horseradish peroxidase (HRP),[3] dioxetane–alkaline phosphatase (ALP)[4] and peroxyoxalate–hydrogen peroxide (H_2O_2)–fluorescent dye[5] have commonly been developed. Due to the difficult modification and poor stability of natural enzymes, the application of some CL systems is limited.[6] Thus new CL systems, including nanoparticle-based CL systems,[7–11] are currently attracting considerable attention.

Recently, some nanocluster enhanced luminol–H_2O_2 CL systems have been developed,[9–11] and oxidant induced quantum dot (QD)–CL systems have also been explored.[12,13] Owing to their wide excitation range, high fluorescence (FL) quantum yield and good optical stability,[14–20] QDs have been considered as a good energy acceptor of luminol donors to produce CL resonance energy transfer (CRET) for indirect CL. This QD–luminol–oxidant system has been used for the development of different sensing systems for thrombin, DNA, ATP, and so on.[21–24] Besides the CRET induced QD CL, electron–hole annihilation (EHA) of nano dots is also a hot topic, in which the nanodots serve as CL emitters to produce enhanced CL from the combination of holes and electron-injected nanodots. For example, CdTe QDs can enhance the CL intensity as well as the lifetime of peroxymonocarbonate (HCO_4^-) by ∼100 times.[25] The high nitrogen-rich QDs enhance the ultra-weak CL of $NaIO_4$ with H_2O_2 by 400-fold.[26] A strong CL of carbon dots has been observed in the presence of peroxynitrous acid and used for sensitive nitrite sensing.[27] These works demonstrate the enhancement of EHA in the CL signal, which leads to the curiosity to exploit new efficient non-enzymatic CL systems of nano dots for amplified biodetection.

Peroxyoxalate CL (PO-CL) is one of the most efficient non-enzyme catalyzed CL reactions.[28] It shows a quantum yield up to 34%, much higher than that of the luminol-based CL system. This work used a bis(2,4,6-trichlorophenyl) oxalate (TCPO)–H_2O_2 CL reaction and CdTe QDs to design a novel CL amplification strategy, CL resonance energy transfer and electron–hole annihilation (CRET/EHA) induced amplification. The strong CL of CdTe QDs in TCPO–H_2O_2 was observed, along with a more durable CL kinetic behavior than the conventional fluorescent dye–TCPO–H_2O_2 system. Using a CdTe QD functionalized microsphere as a detection tag, a sensitive CL immunoassay was exploited *via* the CRET/EHA and 1:*n* amplification.

Mercapto propionic acid (MPA) capped CdTe QDs were synthesized *via* a hydrothermal method. The X-ray photoelectron spectrum (XPS) and transmission electron microscopy (TEM) images showed the successful synthesis of CdTe QDs in a spherical structure with a size of ∼3 nm (Fig. S1A–C, ESI†). The CdTe QDs exhibited a bright orange color under ultraviolet radiation (λ = 365 nm) and a UV-Vis absorption at 540 nm (Fig. S1D, ESI†), which overlapped with the emission region of TCPO–H_2O_2.[29] Thus, the CRET could happen from the oxidation intermediate of TCPO by H_2O_2, 1,2-dioxetanedione (C_2O_4*), to QDs.[30]

While the CdTe QDs–TCPO–H_2O_2 system produced a strong CL, all TCPO–H_2O_2, CdTe QDs–H_2O_2 and CdTe QDs–TCPO systems showed a weak CL (Fig. 1A), indicating that the intermediate species produced by TCPO–H_2O_2 could react with CdTe QDs to yield CL. This CL mechanism could be verified by altering the mixing orders of reagents (Fig. 1B). The highest CL was created with the injection of H_2O_2 into the mixture of CdTe QDs and TCPO because no reaction occurred before the injection.

---

[a] *State Key Laboratory of Analytical Chemistry for Life Science, School of Chemistry and Chemical Engineering, Nanjing University, Nanjing 210023, P. R. China. E-mail: hxju@nju.edu.cn*

[b] *State Key Laboratory of Natural Medicines, China Pharmaceutical University, Nanjing 210009, P. R. China*

† Electronic supplementary information (ESI) available: Experimental section, additional figures and tables. See DOI: 10.1039/c8cc06356g

‡ These authors contributed equally to this work.

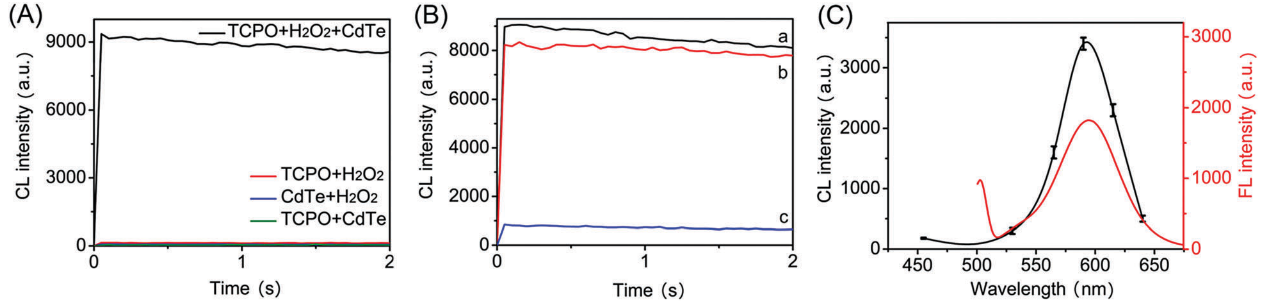

Fig. 1 (A) CL intensity of CdTe QDs–TCPO–H_2O_2, TCPO–H_2O_2, CdTe QDs–H_2O_2 and CdTe QDs–TCPO systems. (B) CL intensity after injecting (a) H_2O_2 into CdTe QDs–TCPO, (b) TCPO into CdTe QDs–H_2O_2, and (c) CdTe QDs into TCPO–H_2O_2. (C) CL spectrum of the CdTe QDs–TCPO–H_2O_2 system with cutoff filters from 420 to 650 nm (black line) and the FL spectrum of CdTe QDs (red line).

The injection of TCPO into the mixture of CdTe QDs and H_2O_2 produced a slightly weaker CL signal, indicating that the product of CdTe QDs–H_2O_2 contributed partially to the CL emission of the CdTe QDs–TCPO–H_2O_2 system. The lowest CL was observed with the injection of CdTe QDs into the mixture of TCPO and H_2O_2 due to the formation and rapid dissociation of the intermediate (C_2O_4*) (reaction (1)).[5,31] These results indicated that the formed C_2O_4* dominated the CL emission of the CdTe QDs–TCPO–H_2O_2 system.

$$R_2C_2O_4\ (\text{TCPO}) + H_2O_2 \rightarrow 2ROH + C_2O_4^* \qquad (1)$$

The CL spectrum displayed the same emission band as the fluorescence (FL) spectrum of CdTe QDs with a peak at 594 nm (Fig. 1C), revealing that the CdTe QDs were the emitting species of the CdTe QDs–TCPO–H_2O_2 CL system.[13,22,23] Similar to the energy transfer between C_2O_4* and a fluorescent dye,[5,31] CRET between C_2O_4* and CdTe QDs produced CdTe* to emit CL (reaction (2)) due to the spectrum matching (Fig. S1D, ESI†).

$$C_2O_4^* + \text{CdTe} \rightarrow \text{CdTe}^* + 2CO_2 \qquad (2)$$

To further investigate the CL mechanism, the whole CL reaction was analyzed using electron paramagnetic resonance (EPR) spectroscopy. 5,5-Dimethyl-1-pyrroline *N*-oxide (DMPO), a specific target molecule of $OH^{\bullet}$, was used to capture and detect the $OH^{\bullet}$ radical.[32,33] As shown in Fig. 2A, H_2O_2 under alkaline conditions could produce $OH^{\bullet}$ and this reaction could be catalyzed by CdTe QDs (reactions (3)–(5)). In addition, the $OH^{\bullet}$ could be stabilized on the surface of QDs.[34,35]

$$H_2O_2 + OH^- \rightarrow HO_2^- + H_2O \qquad (3)$$

$$HO_2^- + H_2O_2 \rightarrow OH^{\bullet} + O_2^{\bullet -} + H_2O \qquad (4)$$

$$H_2O_2 + \text{CdTe (catalyst)} \rightarrow \text{CdTe}(OH^{\bullet})_2 \qquad (5)$$

The $OH^{\bullet}$ radical was consumed greatly in the presence of TCPO, suggesting that the essence of reaction (1) should be the reaction of TCPO with $OH^{\bullet}$ to form C_2O_4* (reaction (6)).

$$R_2C_2O_4 + 2OH^{\bullet} \rightarrow 2ROH + C_2O_4^* \qquad (6)$$

Similarly, the C_2O_4* in the CdTe QDs–TCPO–H_2O_2 system was produced on the surface of CdTe QDs (reaction (7)), resulting in highly efficient collision between C_2O_4* and CdTe QDs to create strong CL.[36]

$$R_2C_2O_4 + \text{CdTe}(OH^{\bullet})_2 \rightarrow 2ROH + \text{CdTe–}C_2O_4^* \qquad (7)$$

2,2,6,6-Tetramethylpiperidine (TEMP), a specific target molecule of $^1O_2$, was also used to identify $^1O_2$.[25,32,33] The results showed that H_2O_2 itself could produce $^1O_2$ (reactions (3), (4) and (8)),[37] and $^1O_2$ existed in all H_2O_2 containing systems (Fig. 2B and Fig. S2, ESI†). However, the addition of CdTe QDs led to a sharp decrease in $^1O_2$, which may be due to the CRET reaction between the CdTe QDs and $^1O_2$ (reaction (9)).

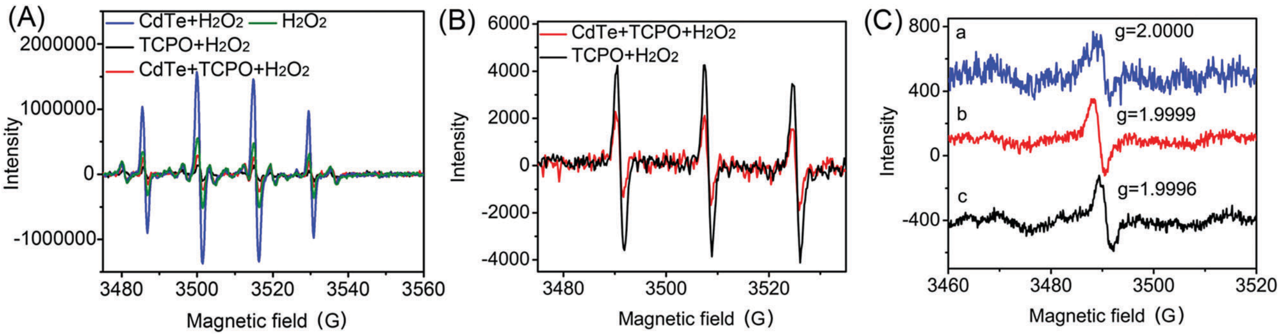

Fig. 2 EPR spectra of (A) $OH^{\bullet}$ radical in H_2O_2, TCPO–H_2O_2, CdTe QDs–H_2O_2 and CdTe QDs–TCPO–H_2O_2 systems, (B) $^1O_2$ in TCPO–H_2O_2 and CdTe QDs–TCPO–H_2O_2 systems, (C) CdTe QDs (a) and CdTe QDs oxidized by H_2O_2 (b) and TCPO–H_2O_2 (c). Experimental conditions: 100 mM TEMP, 100 mM DMPO, 1 μM CdTe QDs, 3.2 mM TCPO, 9.4 mM H_2O_2 containing 1.4 mM imidazole.

Because the CL spectrum of $^1O_2$ (a peak at 634 nm)[38] was far away from the excitation wavelength of CdTe, the efficiency of CRET from $^1O_2$ to CdTe should be much lower than the CRET from C_2O_4* to CdTe.

$$O_2^{\bullet -} + H_2O_2 \rightarrow {}^1O_2 + OH^{\bullet} + OH^{-} \qquad (8)$$

$$^1O_2 + CdTe \rightarrow CdTe^* + O_2 \qquad (9)$$

Effects of different radical scavengers on the CL intensity of the CdTe QDs–TCPO–H_2O_2 system were investigated to identify the action of oxidant species in the CL system (Table S1, ESI†). Ascorbic acid, an effective radical scavenger of $OH^{\bullet}$, was observed to greatly quench the CL signal of the CdTe QDs–TCPO–H_2O_2 system, indicating that $OH^{\bullet}$ played a critical role in the CL emission due to its strong oxidizing ability.[26] In addition, sodium azide (NaN_3), a scavenger for $^1O_2$, was used to identify the effect of $^1O_2$ on the CL emission. The CL intensity of the CdTe QDs–TCPO–H_2O_2 system was slightly quenched by NaN_3, indicating that $^1O_2$ was not the main emitter of the CL system.

EPR was also utilized to study the ground-state properties of CdTe QDs. The CdTe QDs showed an EPR signal at g = 2.0000 (Fig. 2C), suggesting that the ground-state CdTe QDs had a singly occupied orbital and could act as electron donors or electron acceptors during the reaction.[27,39,40] The g-value of CdTe QDs slightly shifted after it reacted with H_2O_2, which explained the low CL of the CdTe–H_2O_2 system. However, after the reaction with TCPO–H_2O_2, the g-value of CdTe QDs was reduced from 2.0000 to 1.9996, revealing the change of the singly occupied orbital in CdTe QDs after the CL emission. Thus, electron–hole annihilation (EHA) was also involved in the CL emission besides the energy transfer (reactions (10)–(13)).

$$C_2O_4^* + CdTe \rightarrow CdTe^{\bullet +} + C_2O_4^{\bullet -} \qquad (10)$$

$$OH^{\bullet} + CdTe \rightarrow CdTe^{\bullet +} + OH^{-} \qquad (11)$$

$$O_2^{\bullet -} + CdTe \rightarrow CdTe^{\bullet -} + O_2 \qquad (12)$$

$$CdTe^{\bullet +} + CdTe^{\bullet -} \rightarrow CdTe^* \qquad (13)$$

Here, C_2O_4*, $OH^{\bullet}$ and $O_2^{\bullet -}$ were formed through the reaction between TCPO and H_2O_2 (reactions (4) and (6)). Although both C_2O_4* and $OH^{\bullet}$ could serve as the hole injectors and convert CdTe QDs to cation radicals $CdTe^{\bullet +}$ (reactions (10) and (11)), the former played the main role. On the other hand, $O_2^{\bullet -}$ could donate an electron to CdTe QDs to produce QDs with a negative charge, $CdTe^{\bullet -}$ (reaction (12)). Finally, electron–hole annihilation in or between the $CdTe^{\bullet +}$ and $CdTe^{\bullet -}$ resulted in the formation of excited CdTe QDs (reaction (13)).

According to the above results and discussion, it could be concluded that CdTe QDs were the main emitters in the CdTe QDs–TCPO–H_2O_2 CL system, and the CL mechanism is shown in Fig. 3. The CL was generated from the energy release of CdTe* (reaction (14)), which was produced by both the CRET between C_2O_4* and the CdTe QDs and the radiative electron–hole annihilation between the hole-injected and electron-injected QDs ($CdTe^{\bullet +}$ and $CdTe^{\bullet -}$). Here, CdTe QDs themselves could catalyze the stable formation of $OH^{\bullet}$ as well as C_2O_4*, hence causing efficient CRET and electron–hole annihilation to generate high CL intensity. The CRET between $^1O_2$ and CdTe QDs was weak and its CL emission could be negligible.

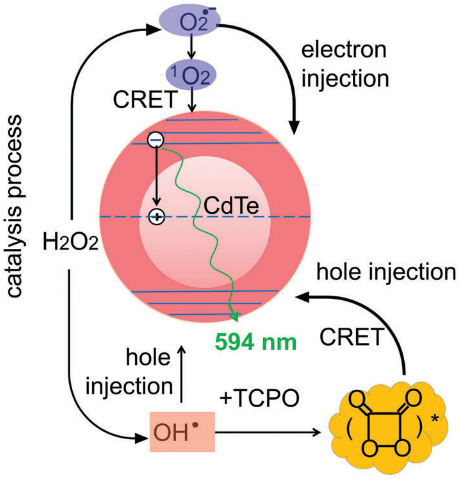

Fig. 3 CL mechanism of the CdTe QDs–TCPO–H_2O_2 system.

$$CdTe^* \rightarrow CdTe + h\nu \qquad (14)$$

The effects of H_2O_2, TCPO and imidazole concentrations on the CdTe QDs–TCPO–H_2O_2 CL system were then examined. Based on the signal-to-noise ratio, 10 mM H_2O_2, 3.4 mM TCPO and 1.5 mM imidazole were used as the optimal conditions (Fig. S3, ESI†). Under these conditions, the CL intensity increased with increasing CdTe QD concentration from 7.2 nM to 600 nM, and a linear relationship was observed under 150 nM (Fig. S4, ESI†). In addition, common ions and surfactants had little effect on this CdTe QDs–TCPO–H_2O_2 CL system (Table S1, ESI†). Furthermore, the CdTe QDs–TCPO–H_2O_2 CL system exhibited a more durable CL kinetic behavior than the common TCPO–H_2O_2–Cy5 CL system[41] (Fig. S5, ESI†). All these results indicated the good feasibility of the proposed CdTe QDs–TCPO–H_2O_2 CL system for bioanalysis.

A sensitive CL immunoassay was further constructed for demonstrating the application of the CdTe QDs–TCPO–H_2O_2 CL system for signal readout. The immunoassay was performed on a home-made anti-CEA glass chip. After a sandwich-based target recognition experiment, an avidin modified polystyrene (PS) microsphere along with an amount of biotin modified CdTe QDs was captured on each sandwich immunocomplex *via* avidin–biotin conjugation to perform the 1:n amplification (Fig. S6A, ESI†). After the addition of TCPO and H_2O_2, the CdTe QDs captured on the protein chip could produce a CL signal. The PS assisted CL system produced 2.3 times higher CL emission than that without the PS microsphere, along with similar noise (Fig. S7, ESI†). With the increasing concentration of CEA, more CdTe QDs could be captured, resulting in the stronger CL signal (Fig. S6B, ESI†). In this CL immunoassay, the CL intensity was proportional to the logarithm value of the CEA concentration over the range of 0.1 ng mL^{-1} to 10 μg mL^{-1} (Fig. S6C, ESI†). The limit of detection corresponding to the CL signal of 3SD was 0.092 ng mL^{-1} ($\sim$0.3 pM). The low detection limit and the wide detection range were comparable to those of the sensitive CL immunoassays based on HRP or other mimicking enzymes (Table S2, ESI†). Furthermore, the cross-reactivity and nonspecific binding among analytes and nonspecific antibodies were demonstrated to be negligible (Fig. S6D, ESI†). The assay results of CEA in 7 human serum samples from healthy people and cancer patients obtained using the proposed CL immunoassay method were in good agreement with the reference values obtained *via* commercial ECL single-analyte testing, with relative errors less than 6.3% (Table S3, ESI†), indicating the good accuracy of the immunoassay using the CdTe QDs–TCPO–H_2O_2 CL system.

Theoretically, a wide scope of biomarkers which have the corresponding sandwich recognition can satisfy the proposed method. Using alpha fetoprotein (AFP) as another model, the novel CdTe QDs–TCPO–H_2O_2 CL system could conveniently be extended by easily alternating the antibodies. Under the optimal conditions, the linear range for AFP detection was from 0.05 ng mL^{-1} to 10.5 μg mL^{-1} and the detection limit was 0.035 ng mL^{-1} ($\sim$0.5 pM) (Fig. S8, ESI†).

In conclusion, CdTe QDs can act as the CL emitter to produce strong signal readout in the presence of TCPO and H_2O_2. The CL emission is demonstrated to undergo two pathways: CRET and radiative electron–hole annihilation between hole- and electron-injected QDs. The exploration of CdTe QD CL shows important significance in amplifying the detection signal for sensitive enzyme-free bioanalysis and the development of nanoparticle-based CL systems. The designed CRET/EHA amplification strategy can be further combined with 1:*n* amplification by easily assembling the QDs on a microsphere to act as a tag. As a proof-of-concept, the tag has been used for the development of a sensitive CL immunoassay method. The high sensitivity, wide detection range, acceptable selectivity, good versatility and accuracy show good practicability of the CdTe QDs–TCPO–H_2O_2 CL system.

One thing to be noted is that the CdTe QDs–TCPO–H_2O_2 CL system is a flash-type CL. For high-throughput cancer diagnosis using 96-well microplates, glow-type CL has more advantages. To be more practical, more QD-based CL systems with glow-type CL should be further developed.

The authors would like to acknowledge the National Natural Science Foundation of China (21505160, 21635005, and 21575063), the Natural Science Foundation of Jiangsu Province (BK20150690) and Independent Research Foundation from the State Key Laboratory of Analytical Chemistry for Life Sciences (5431ZZXM1807).

Conflicts of interest

There are no conflicts to declare.

References

1 A. Kunze, M. Dilcher, A. A. Wahed, F. Hufert, R. Niessner and M. Niessner, *Anal. Chem.*, 2016, **88**, 898–905.
2 S. Bi, S. Z. Yue, W. L. Song and S. S. Zhang, *Chem. Commun.*, 2016, **52**, 12841–12844.
3 X. G. Li, M. Meng, L. Zheng, Z. H. Xu, P. Song, Y. M. Yin, S. A. Eremin and R. M. Xi, *Anal. Chem.*, 2016, **88**, 8556–8561.
4 Z. J. Hai, J. D. Li, J. J. Wu, J. C. Xu and G. L. Liang, *J. Am. Chem. Soc.*, 2017, **139**, 1041–1044.
5 Y. D. Lee, C. K. Lim, A. Singh, J. Koh, J. Kim, I. C. Kwon and S. Kim, *ACS Nano*, 2012, **6**, 6759–6766.
6 W. R. Algar, M. Massey and U. J. Krull, *TrAC, Trends Anal. Chem.*, 2009, **28**, 292–306.
7 H. Cui, Z. F. Zhang, M. J. Shi, Y. Xu and Y. L. Wu, *Anal. Chem.*, 2005, **77**, 6402–6406.
8 W. Liu, J. Luo, M. Zhao, H. F. Li and B. X. Li, *Anal. Bioanal. Chem.*, 2016, **408**, 8821–8830.
9 Y. Y. Sheng, H. L. Yang, Y. Wang, L. Han, Y. J. Zhao and A. P. Fan, *Talanta*, 2017, **166**, 268–274.
10 M. Deng, S. J. Xu and F. N. Chen, *Anal. Methods*, 2014, **6**, 3117–3123.
11 S. J. Xu, F. N. Chen, M. Deng and Y. Y. Sui, *RSC Adv.*, 2014, **4**, 15664–15670.
12 S. K. Poznyak, D. Talapin, E. Shevchcnko and H. Weller, *Nano Lett.*, 2004, **4**, 693–698.
13 Z. Wang, J. Li, B. Liu and J. J. Li, *J. Phys. Chem. C*, 2005, **109**, 23304–23311.
14 Y. D. Yin and A. P. Alivisatos, *Nature*, 2005, **437**, 664–670.
15 C. Burda, X. B. Chen, R. Narayanan and M. A. El-Sayed, *Chem. Rev.*, 2005, **105**, 1025–1102.
16 Y. T. Long, C. Kong, D. W. Li, Y. Li, S. Chowdhury and H. Tian, *Small*, 2011, **7**(12), 1624–1628.
17 W. Ma, L. X. Qin, F. T. Liu, Z. Gu, J. Wang, Z. G. Pan, T. D. James and Y. T. Long, *Sci. Rep.*, 2013, **3**, 1537.
18 L. X. Qin, W. Ma, D. W. Li, Y. Li, X. Y. Chen, H. Kraatz, T. D. James and Y. T. Long, *Chem. – Eur. J.*, 2011, **17**, 5262–5271.
19 W. Ma, H. T. Liu, X. P. He, Y. Zhang, J. Li, G. R. Chen, H. Tian and Y. T. Long, *Anal. Chem.*, 2014, **86**, 5502–5507.
20 W. H. Zhang, W. Ma and Y. T. Long, *Anal. Chem.*, 2016, **88**, 5131–5136.
21 X. Huang, L. Li, H. Qian, C. Dong and J. Ren, *Angew. Chem., Int. Ed.*, 2006, **45**, 5140–5143.
22 S. X. Xu, X. M. Li, C. B. Li, J. L. Li, X. F. Zhang, P. Wu and X. D. Hou, *Anal. Chem.*, 2016, **88**, 6418–6424.
23 R. Freeman, X. Liu and I. Willner, *J. Am. Chem. Soc.*, 2011, **133**, 11597–11604.
24 X. Q. Liu, R. Freeman, E. Golub and I. Willner, *ACS Nano*, 2011, **5**, 7648–7655.
25 H. Chen, L. Lin, Z. Lin, G. S. Guo and J. M. Lin, *J. Phys. Chem. A*, 2010, **114**, 10049–10058.
26 Y. Z. Zheng, D. K. Zhang, S. N. A. Shah, H. F. Li and J. M. Lin, *Chem. Commun.*, 2017, **53**, 5657–5660.
27 L. Zhen, X. Wei, H. Chen and J. M. Lin, *Anal. Chem.*, 2011, **83**, 8245–8251.
28 S. S. Tseng, A. G. Mohan, L. G. Haines, L. S. Vizcarra and M. M. Rauhut, *J. Org. Chem.*, 1979, **44**, 4113–4116.
29 B. Mann and M. L. Grayeski, *Anal. Chem.*, 1990, **62**, 1532–1536.
30 J. Y. Koo and G. B. Schuster, *J. Am. Chem. Soc.*, 1977, **99**, 6107–6109.
31 D. W. Lee, S. Khaja, J. C. Velasquez-Castano, M. Dasari, C. Sun, J. Petros, W. R. Taylor and N. Murthy, *Nat. Mater.*, 2007, **6**, 765–769.
32 H. Chen, H. F. Li and J. M. Lin, *Anal. Chem.*, 2012, **84**, 8871–8879.
33 H. Chen, R. B. Li, H. F. Li and J. M. Lin, *J. Phys. Chem. C*, 2012, **116**, 14796–14803.
34 S. N. A. Shah, Y. Z. Zheng, H. F. Li and J. M. Lin, *J. Phys. Chem. C*, 2016, **120**, 9308–9316.
35 S. F. Li, X. M. Zhang, W. X. Du, Y. H. Ni and X. W. Wei, *J. Phys. Chem. C*, 2009, **113**, 1046–1051.
36 S. F. Li, X. Z. Li, Y. Q. Zhang, F. Huang, F. F. Wang and X. W. Wei, *Microchim. Acta*, 2009, **167**, 103–108.
37 Y. X. Li, P. Yang, P. Wang, X. Huang and L. Wang, *Nanotechnology*, 2007, **18**, 225602.
38 C. Lu and J. M. Lin, *Catal. Today*, 2004, **90**, 343–347.
39 D. Y. Pan, J. C. Zhang, Z. Li, C. Wu, X. M. Yan and M. H. Wu, *Chem. Commun.*, 2010, **46**, 3681–3683.
40 X. Wang, L. Cao, F. S. Lu, M. J. Meziani, H. T. Li, G. Qi, B. Zhou, B. A. Harruff, F. Kermarrec and Y. P. Sun, *Chem. Commun.*, 2009, 3774–3776.
41 C. Zong, J. Wu, M. M. Liu, L. L. Yang, L. Liu, F. Yan and H. X. Ju, *Anal. Chem.*, 2014, **86**, 5573–5578.